Supplemental Material

Animals

Nine to 11 weeks old C57BL/6J mice (Jackson lab, n=30) of both genders were used in all the studies. The Johns Hopkins University Institutional Animal Care and Use Committee approved all animal experiments. Transverse Aortic Constriction was performed through the Cardiac Physiology Core in the Division of Cardiology at Johns Hopkins University as previously described[1].

Human Samples

Consent for biopsy procedure and the use of myocardial tissue was prospectively obtained in all cases. Ischemic, dilated (non-ischemic) and control cardiac tissues were collected and stored as previously described[2].

Lentivirus Production

Desmin cDNA was obtained from RNA isolated from the NRVMs to account for strain single nucleotideploymorphisms. Desmin-GFP phospho-mimetic/null mutants (Ser, S to Ala, A or Asp, D for Ser-27 and -31 residues, mature sequence) were obtained by PCR using mutated primers, subcloned into lentiviral vectors downstream of a CMV promoter and expanded into human embryonic kidney (HEK) 293T cells, transduced by calcium-phosphate co-precipitation. The supernatant from the flask was collected 48 and 72 hours after transfection, sterilized and concentrated by ultrafiltration. The concentrated lentiviral stock was applied to freshly isolated NRVMs in the presence of 8 μg/ml of Polybrene (Sigma-Aldrich) for 48 hrs. The human desmin clone was purchased at Origene (homo sapiens DESMIN (DES) as transfection-ready DNA NM_001927.3). Desmin mutants (Ser to Ala and Ser to Glu for both residues 27 and 31, and combination) was produced by PCR of the mutated primers.

Protein Biochemistry

Protein samples from frozen tissue were obtained by crushing the frozen samples using a frozen, hand-held, impact device cooled in dry-ice. Precisely weighted 30-50 mg of tissue crumbles were either hand homogenized or further pulverized by means of a mixer mill Retsch #MM400) cooled in liquid nitrogen (25 Hz for 1', twice). The resulting powder was re-suspended in 25 mM Hepes pH=7.4, completed with protease (Mini, Roche) and phosphatase (Phos-stop, Sigma) inhibitors and further processed as described previously[3]. For Western blot analysis the anti-desmin antibody (DE-U-10, Sigma) was used at a 1:10,000 dilution whereas the A11 provide by its creator Dr. Charles Glabe, and the anti-cryAB (SPA-223, Stressgen) antibodies were used at a 1:2500 dilution in 5% milk (Carnation Instant Nonfat, Nestle) in 0.1% Tween 20/ Tris-Buffered Saline (TBS-T). Ten µg of protein per lane were separated using precast gels (NuPAGE 3-12% gels, Life Technologies), followed by wet blotting on nitrocellulose (Bio-Rad). The resulting blots were incubated in the A11 over-night. LI-COR® species-specific secondary antibodies (goat red anti-mouse and green anti-rabbit) were 1:15,000 -1:30,000 diluted in 5% milk in TBS-T and used for detection. Membranes were further stripped to remove the excess of milk (Restore, Pierce) and stained with direct blue 71 (DB71, Sigma) to assess protein load and transfer efficiency. The Thioflavin T stain was optimized for classical SDS-PAGE as described (*manuscript in preparation*). Mass spectrometry analysis on in-gel digested samples was performed on an Orbitrap (Thermo). Spectra were searched and analyzed using Scaffold (Proteome Software).

Filter Assay

We combined Thioflavin T stain with this approach. Briefly, protein homogenates (5 µg of total protein/sample) were filtered through a nitrocellulose membrane (0.2 µM cut-off, Bio-Rad) using a dot-blot apparatus (Bio-Rad) in the presence of 2% SDS. For desmin aggregate quantitation, the membrane was treated as described in the western blot analysis section using the DE-E-10 antibody. After antibody detection the membrane was stripped using Retsore ® (Pierce) followed by staining with Direct Blue 71. Membrane image was therefore acquired using a Typhoon Trio laser scanner (GE Healthcare) to detect auto fluorescence, following by incubation with a 0.1% Thioflavin T solution for 1 hr, RT. After several washes the signal of Thioflavin T was recorded using the Typhoon. Densitometry

on the exported .tif image was performed on background subtracted, inverted images suing the circular selection tool in the Image J package Fiji.

Animal PET, SPECT and Euthanasia

We used the relatively long-lived and FDA approved [^{18}F] Fluorbetapir (Amyvid®, Ely Lilly), which enables the injection of several mice in the same experiment due to its extended half-life, with a considerable cost benefit. Mice were anesthetized with 2.5% isofluorane in oxygen, weighed, then injected with 200 µCi of Amyvid® in 200 µl of saline, via a catheter placed in the tail vein. After 10 min to allow cardiac up-take of the tracer, mice were scanned for 20 min using ungated dynamic acquisition in listmode. PET imaging was performed using a GE eXplore Vista small animal PET scanner, imaging two mice (treated and control) concurrently; images were analyzed using the software package PMOD (v 3.3, PMOD Technologies Ltd, Zurich, Switzerland). First, reconstructed PET images were co-registered with the CT images of the same mice, and anatomical regions-of-interest (ROIs) of hearts defined. These ROIs were transferred to the PET data, and mean heart Amyvid® uptakes for each experimental group calculated. To minimize inconsistencies and potential confounding factors, treated groups were always paired with suitable controls using the same batch of radio-tracers, imaging protocols, and under identical animal prep conditions. After normalizing for injected dose and body weight, cardiac Amyvid® uptake ratios between each pair of treated and control mice were used to quantify the differences between them. After the PET scan, a subgroup of mice were euthanized using a lethal dose of pentobarbital to allow motion-free CT scanning using a Gamma Medica small X-SPECT imager.

Magnetic twisting cytometry (MTC)

Magnetic twisting cytometry is based on ferromagnetic microbeads (4.5 µm in diameter) coated with a synthetic peptide containing the sequence arginine-glycine-aspartic acid (RGD). Such RGD-coated beads bind avidly to the integrin receptors present on the cell surface, form focal adhesions and

become well-integrated into the cytoskeletal scaffold[4, 5]. The bead is magnetized horizontally and then twisted in a vertically-aligned homogeneous magnetic field that is varying sinusoidally with time. This sinusoidal twisting field causes both a rotation and a pivoting displacement of the bead. As the bead moves, it exerts stress upon cytoskeletal structures deep in the cell interior, and such *forced* bead motions are, in turn, impeded by elastic and frictional properties of the underlying cytoskeleton within the cell body[4-6]. Here, the ratio of specific torque to lateral bead displacements is taken as a measure of complex elastic modulus g*, and is expressed in units of Pascal per nanometer (Pa/nm). As defined previously, the complex elastic modulus of the cell $g^*(f)=g'(f)+ig''(f)$ has two parts: the real part (the storage modulus *g'*) and the imaginary part (the loss modulus *g"*). The storage modulus *g'* reflects the stored elastic energy or stiffness, whereas the loss modulus *g"* reflects the dissipated mechanical energy or internal friction[7].

For the experiment described in this study, 30.000 NRVMs/well were plated in 96 well multiwell plate previously coated with 0.5% gelatin (Sigma). In order to rule out any contribution provided by the inherent contraction of NRVMs cultures, the contraction uncoupler heptanol (2 mM, 5 minutes)[8] was used. The day of MTC measurement cells were incubated with the beads at a 1:1 ratio, and displacement was measured using a microscope equipped with a camera and tracking system. An average of 205±53SD cells per data point were imaged.

References to Supplementary Methods

1. Kaludercic N, Carpi A, Nagayama T, Sivakumaran V, Zhu G, Lai EW, Bedja D, De Mario A, Chen K, Gabrielson KL, Lindsey ML, Pacak K, Takimoto E, Shih JC, Kass DA, Di Lisa F and Paolocci N. Monoamine oxidase B prompts mitochondrial and cardiac dysfunction in pressure overloaded hearts. *Antioxid Redox Signal*. 2014;20:267-80.
2. Lee DI, Zhu G, Sasaki T, Cho GS, Hamdani N, Holewinski R, Jo SH, Danner T, Zhang M, Rainer PP, Bedja D, Kirk JA, Ranek MJ, Dostmann WR, Kwon C, Margulies KB, Van Eyk JE, Paulus WJ, Takimoto E and Kass DA. Phosphodiesterase 9A controls nitric-oxide-independent cGMP and hypertrophic heart disease. *Nature*. 2015;519:472-6.
3. Agnetti G, Halperin VL, Kirk JA, Chakir K, Guo Y, Lund L, Nicolini F, Gherli T, Guarnieri C, Caldarera CM, Tomaselli GF, Kass DA and Van Eyk JE. Desmin modifications associate with amyloid-like oligomers deposition in heart failure. *Cardiovasc Res*. 2014;102:24-34.
4. An SS, Kim J, Ahn K, Trepat X, Drake KJ, Kumar S, Ling G, Purington C, Rangasamy T, Kensler TW, Mitzner W, Fredberg JJ and Biswal S. Cell stiffness, contractile stress and the role of extracellular matrix. *Biochem Biophys Res Commun*. 2009;382:697-703.

5. Fabry B, Maksym GN, Butler JP, Glogauer M, Navajas D and Fredberg JJ. Scaling the microrheology of living cells. *Phys Rev Lett*. 2001;87:148102.
6. Trepat X, Deng L, An SS, Navajas D, Tschumperlin DJ, Gerthoffer WT, Butler JP and Fredberg JJ. Universal physical responses to stretch in the living cell. *Nature*. 2007;447:592-5.
7. Laudadio RE, Millet EJ, Fabry B, An SS, Butler JP and Fredberg JJ. Rat airway smooth muscle cell during actin modulation: rheology and glassy dynamics. *Am J Physiol Cell Physiol*. 2005;289:C1388-95.
8. Kimura H, Oyamada Y, Ohshika H, Mori M and Oyamada M. Reversible inhibition of gap junctional intercellular communication, synchronous contraction, and synchronism of intracellular Ca2+ fluctuation in cultured neonatal rat cardiac myocytes by heptanol. *Exp Cell Res*. 1995;220:348-56.

Online Table I: Echocardiographic and organ gravimetric parameters in sham and TAC animals.

	Sham			**TAC**			***P*-value**
	Mean	**SEM**	**N**	**Mean**	**SEM**	**N**	
LVEDD (mm)	2.9	0.02	10	3.6	0.18	10	0.002
LVESD (mm)	1.2	0.01	10	2.3	0.24	10	0.000
IVSD (mm)	0.9	0.02	10	1.2	0.02	10	0.000
LVPWD (mm)	0.9	0.01	10	1.2	0.02	10	0.000
FS (%)	58	0.2	10	36	3.6	10	0.000
Echo LV mass (mg)	84	1.6	10	168	13.1	10	0.000
Heart weight / TL (mg/mm)	6.73	0.314	7	10.87	1.477	7	0.018
Lung weight / TL (mg/mm)	7.27	0.296	7	9.55	0.480	7	0.002

LVEDD: left ventricular end-diastolic diameter; LVESD: left ventricular end-systolic diameter; IVSD: interventricular septum end-diastolic diameter; LVPWD: left ventricular posterior wall end-diastolic diameter; FS: fractional shortening; LV: left ventricle; TL: tibia length.
P-values were calculated by two-tailed Student's *t*-test.

Legends to Online Figures

Online Figure I. Desmin fragment detection in TAC mice by 1DE/Mass Spectrometry. Presence of desmin in the ≈45-50 kDa range was determined by 1DE combined by mass spectrometry (MS). A Coomassie brilliant blue (CBB)-stained gel image, highlighting the regions selected for MS analysis, is shown in panel **A**. After reduction, alkylation and digestion, extracted peptides were analyzed by MS. Sequence coverage for desmin in the excised bands is shown in panel **B** and **C**.

Online Figure II. Desmin PAOs by Thioflavin T staining and Mass Spectrometry in R120G cryAB mice. Presence of desmin in the ThT-positive band at ≈55 kDa was determined by mass spectrometry. Coomassie brilliant blue (CBB) and ThT stain of the ≈55 kDa are shown in panel **A**. The CBB stain allowed to locate and excise the ThT-positive band with the naked eye. After reduction, alkylation and digestion, extracted peptide were analyzed by MS. Sequence coverage for desmin in the excised ≈55 kDa ThT-positive band is shown in panel **B**, whereas a representative spectrum of the peptide TFGGAPGFSLGSPLSSPVFPRA is shown in panel **C**.

Online Figure III. NRVMs efficiently express desmin phospho-mimetic mutants. Our lentiviral construct was able to reliably induce WT and mutant desmin expression that can be conveniently measured by western blot analysis using a desmin antibody (DE-U-10, Sigma). Exogenous and endogenous desmin can be separated because of the GFP tag fused with exogenous desmin. Panel A provides a representative image of western blot of protein extracts from NRVMs transduced with WT and phospho-mimetic desmin, DD and AD as well as non-transduced (NT) cells. In panel B a representative densitometry profile highlighting the separation of differently modified and mutant desmin-GFP. Ubiquitinated desmin was predicted based on molecular weight (MW).

Online Figure IV. Biophysical measurements in transduced NRVMs. The average frequency of contraction per field was measured during the live imaging experiments (**A**). Cell stiffness was measured in transduced NRVMs as described in detail in the supplementary methods section (**B**).

Online Figure V. Desmin PAOs by Thioflavin T staining and Mass Spectrometry in TAC mice. Presence of desmin in the ThT-positive band at ≈190 kDa was determined by mass spectrometry. Coomassie brilliant blue (CBB) and ThT stain of the ≈190 kDa are shown in panel **A**. The CBB stain enabled us to locate and excise the ThT-positive band with the naked eye. After reduction, alkylation and digestion, extracted peptide were analyzed by MS. Sequence coverage for desmin in the excised

≈190 kDa-positive band is shown in panel **B**, whereas a representative spectrum of the peptide TFGGAPGFSLGSPLSSPVFPRA is shown in panel **C**. Interestingly, the N-term of desmin seems to be over-represented in this band.

Online Figure I

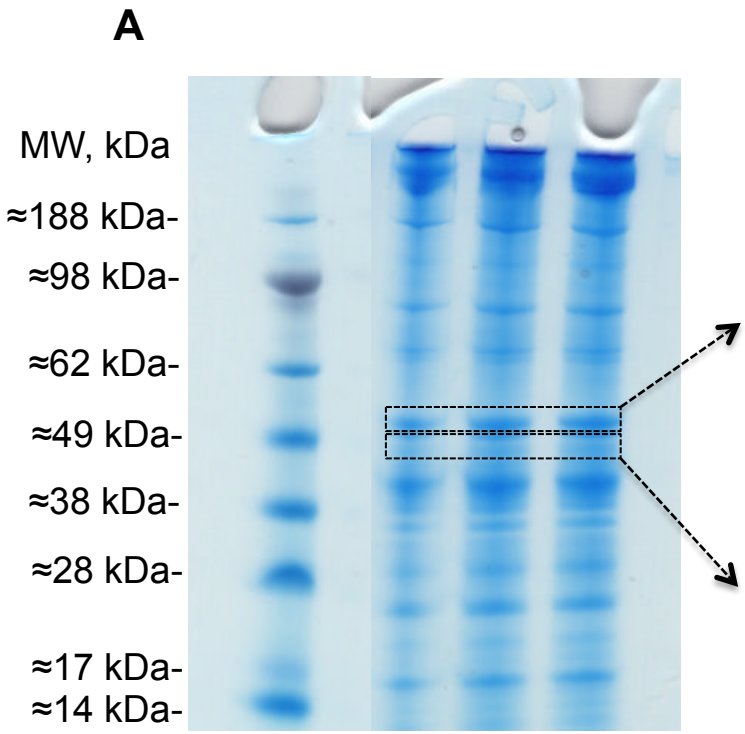

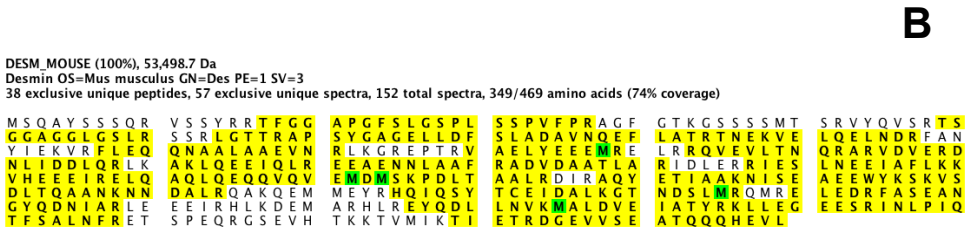

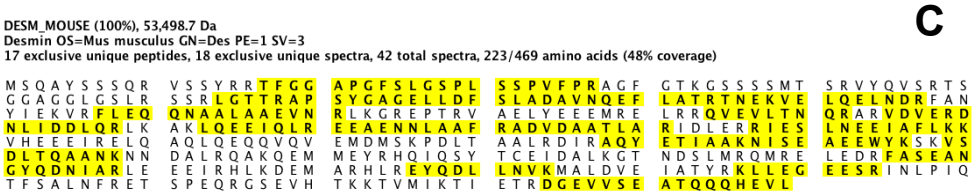

Online Figure II

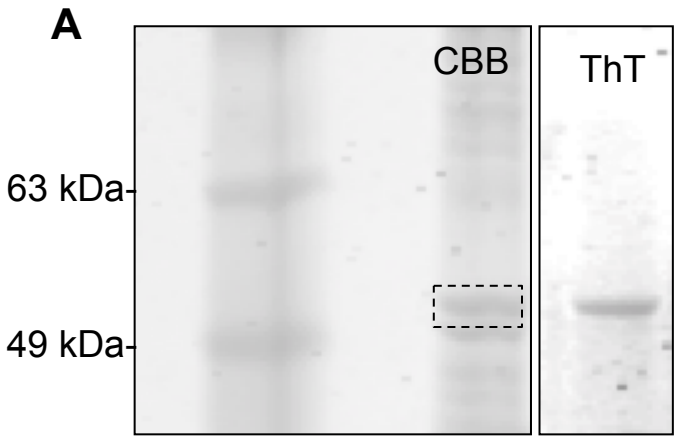

B

DESM_MOUSE (100%), 53,498.7 Da
Desmin OS=Mus musculus GN=Des PE=1 SV=3
31 exclusive unique peptides, 42 exclusive unique spectra, 111 total spectra, 330/469 amino acids (70% coverage)

MSQAYSSSQR	VSSYRRTFGG	APGFSLGSPL	SSPVFPRAGF	GTKGSSSSMT	SRVYQVSRTS	
GGAGGLGSLR	SSRLGTTRAP	SYGAGELLDF	SLADAVNQEF	LATRTNEKVE	LQELNDRFAN	
YIEKVRFLEQ	QNAALAAEVN	RLKGREPTRV	AELYEEEMRE	LRRQVEVLTN	QRARVDVERD	
NLIDDLQRLK	AKLQEEIQLR	EEAENNLAAF	RADVDAATLA	RIDLERRIES	LNEEIAFLKK	
VHEEEIRELQ	AQLQEQQVQV	EMDMSKPDLT	AALRDIRAQY	ETIAAKNISE	AEEWYKSKVS	
DLTQAANKNN	DALRQAKQEM	MEYRHQIQSY	TCEIDALKGT	NDSLMRQMRE	LEDRFASEAN	
GYQDNIARLE	EEIRHLKDEM	ARHLREYQDL	LNVKMALDVE	IATYRKLLEG	EESRINLPIQ	
TFSALNFRET	SPEQRGSEVH	TKKTVMIKTI	ETRDGEVVSE	ATQQQHEVL		

C

TFGGAPGFSLGSPLSSPVFPRA

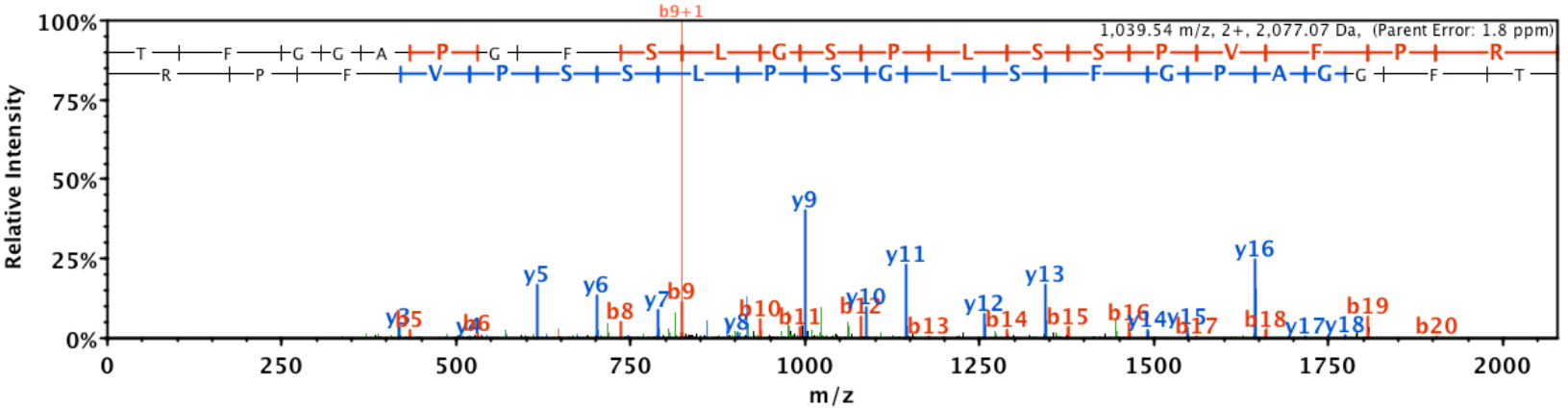

Online Figure III

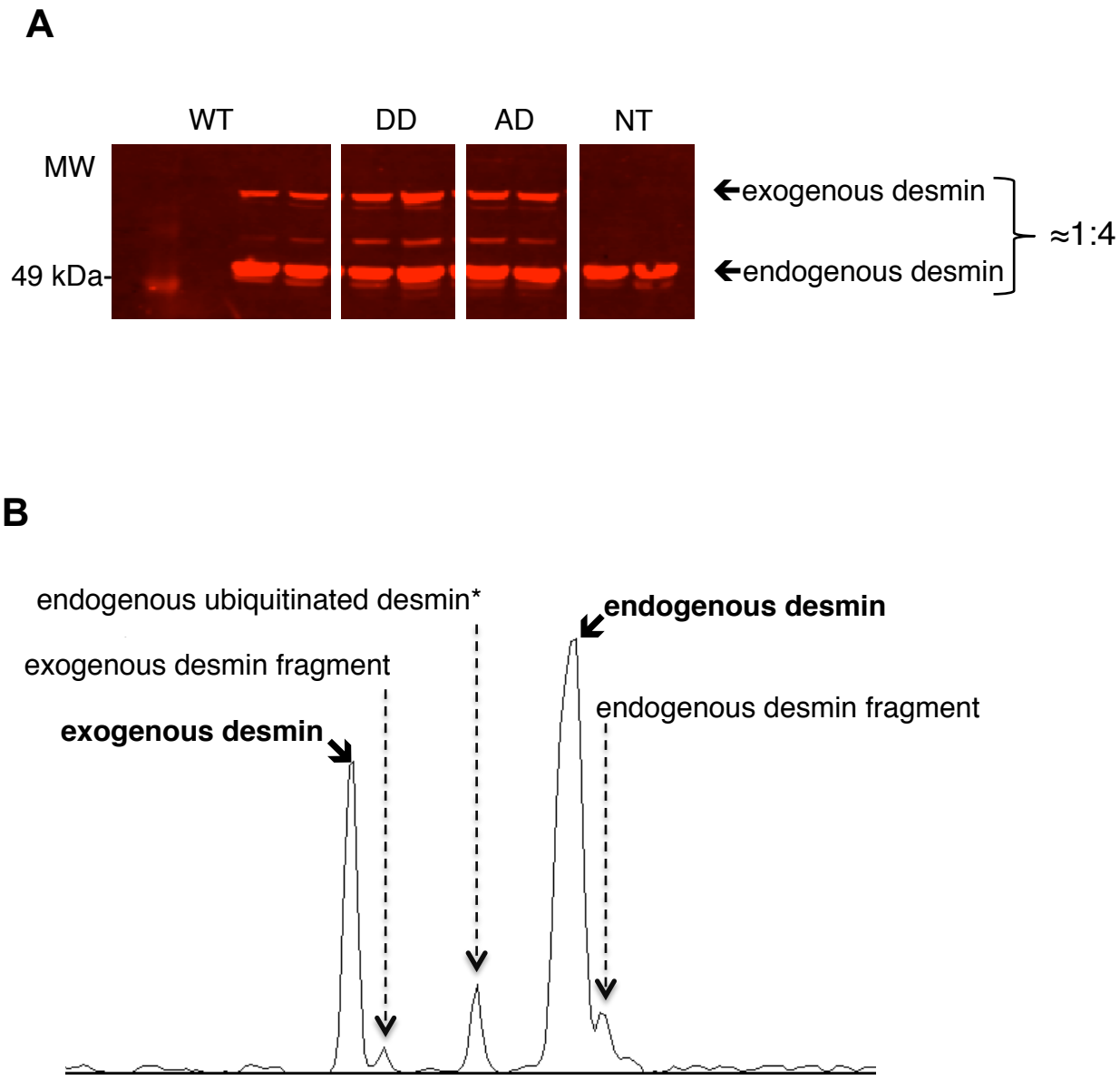

Online Figure IV

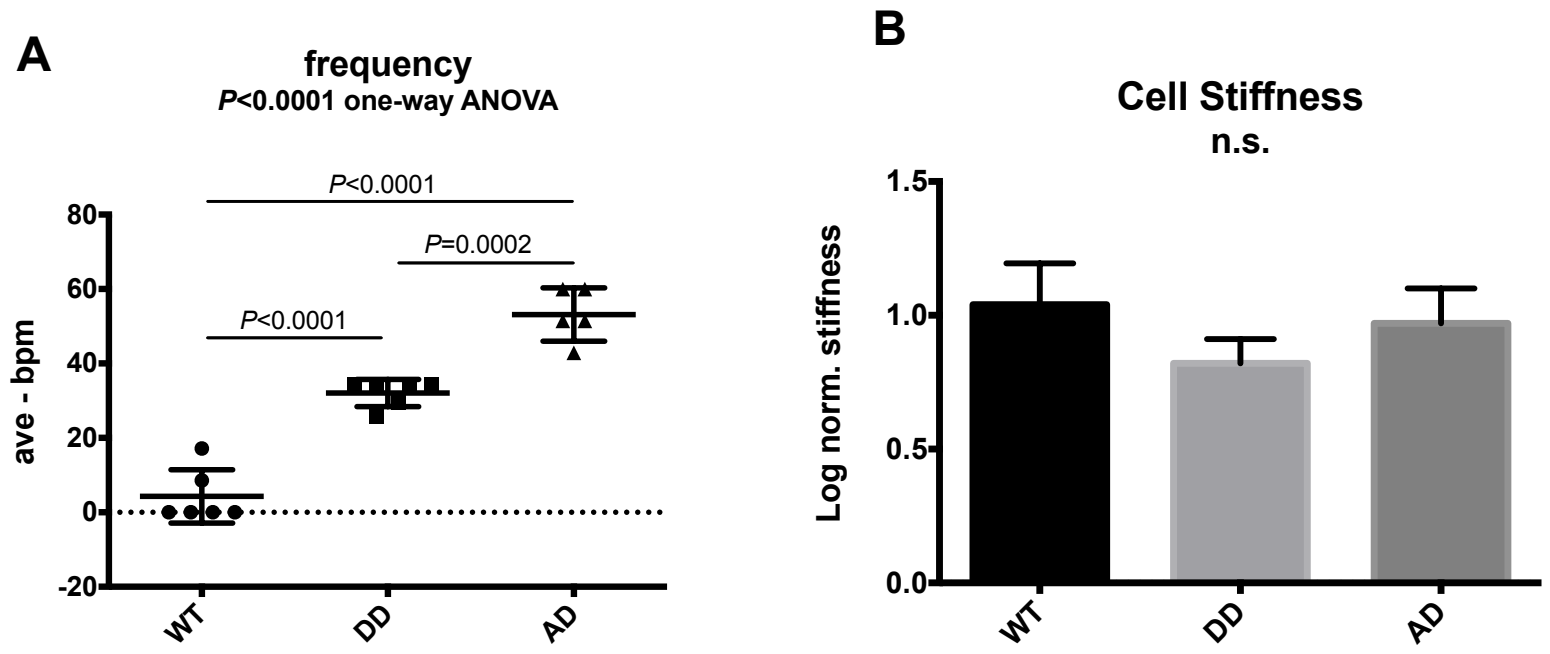

Online Figure V

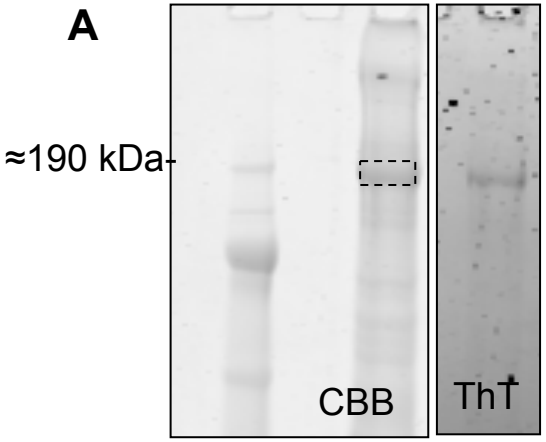

B

DESM_MOUSE (100%), 53,498.7 Da
Desmin OS=Mus musculus GN=Des PE=1 SV=3
3 exclusive unique peptides, 3 exclusive unique spectra, 6 total spectra, 54/469 amino acids (12% coverage)

MSQAYSSSQR	VSSYRRTFGG	APGFSLGSPL	SSPVFPRAGF	GTKGSSSSMT	SRVYQVSRTS		
GGAGGLGSLR	SSRLGTTRAP	SYGAGELLDF	SLADAVNQEF	LATRTNEKVE	LQELNDRFAN		
YIEKVRFLEQ	QNAALAAEVN	RLKGREPTRV	AELYEEEMRE	LRRQVEVLTN	QRARVDVERD		
NLIDDLQRLK	AKLQEEIQLR	EEAENNLAAF	RADVDAATLA	RIDLERRIES	LNEEIAFLKK		
VHEEEIRELQ	AQLQEQQVQV	EMDMSKPDLT	AALRDIRAQY	ETIAAKNISE	AEEWYKSKVS		
DLTQAANKNN	DALRQAKQEM	MEYRHQIQSY	TCEIDALKGT	NDSLMRQMRE	LEDRFASEAN		
GYQDNIARLE	EEIRHLKDEM	ARHLREYQDL	LNVKMALDVE	IATYRKLLEG	EESRINLPIQ		
TFSALNFRET	SPEQRGSEVH	TKKTVMIKTI	ETRDGEVVSE	ATQQQHEVL			

C